ACS chemical biology

LETTER

Simultaneous Recording of Multiple Cellular Events by FRET

Alen Piljic and Carsten Schultz*

Gene Expression Unit, European Molecular Biology Laboratory, Meyerhofstr. 1, 69117 Heidelberg, Germany

ABSTRACT The function of many sensors for measuring intracellular events is based on Förster resonance energy transfer (FRET). Here we demonstrate for the first time the use of multiple ratiometric FRET sensors in parallel through spatial and spectral resolution. We monitored three calcium-dependent signaling events by a cytosolic sensor for calcium/calmodulin-dependent protein kinase IIα, a membrane-bound sensor for protein kinase C, and a translocating FRET probe based on annexin A4. This multiparameter imaging approach gives insight into the precise timing of cellular events within one single cell, thereby providing a major advantage over single-parameter protocols. This type of imaging will likely be important for high content cell analysis and screening efforts in the future.

*Corresponding author, schultz@embl.de.

Received for review November 30, 2007 and accepted January 30, 2008.

Published online March 20, 2008

10.1021/cb700247q CCC: $40.75

© 2008 American Chemical Society

After the introduction of the green fluorescent protein (GFP) and its spectral derivatives in cell biology, Förster resonance energy transfer (FRET) sensors became popular tools for studying intracellular processes (*1*–*5*). Although such sensors have the potential of uncovering a wealth of cellular information, it is a challenge to study several processes in a single cell at the same time (*6*). Multicolor FRET approaches have been described for analysis of protein interactions (*7*, *8*). However, imaging of more than one ratiometric FRET sensor in conventional fluorescence microscopy remains complicated, because most of the sensors designed up to now are based on cyan (CFP) and yellow (YFP) fluorescent proteins and their readouts are therefore spectrally impossible to separate.

To expand the spectral diversity of FRET sensors, we here describe a novel FRET sensor based on mOrange and mCherry fluorescent proteins (ORNEX4) that detects calcium-dependent annexin A4 self-association on membrane surfaces similarly to the previously described sensor CYNEX4 that is based on FRET between CFP and YFP (*9*). mCherry and mOrange are fluorescent proteins that were previously used as a FRET pair (*10*). From a spectral point of view an mOrange−mCherry sensor is easily combined with CFP−YFP FRET sensors. To evaluate the technical limits of multiple FRET sensor usage, the goal was to monitor self-association of annexin A4 in combination with not one but two cyan−yellow FRET sensors in a biologically useful fashion. One of the two CFP−YFP sensors measured activation of the cytosolic calcium/calmodulin-dependent protein kinase IIα (CaMKIIα), while the other enabled visualization of protein kinase C (PKC) activity at the plasma membrane. Annexin A4, CaMKIIα, and PKC are all sensitive to calcium binding directly or indirectly via calmodulin in the case of CaMKIIα. All three proteins are part of the same signaling pathway that regulates calcium-activated chloride conductance (CaCC) in epithelial cells. Specifically, the kinases are believed to enhance CaCC, whereas annexin A4 was reported to inhibit it (*11*, *12*). This suggested a difference in timing of kinase activation and annexin A4 self-association, which would allow the CaCC to be transiently activated, as is observed by electrophysiological experiments (*13*). If such difference is small, it might only be observed if all three sensors are combined and analyzed in the same cell.

The ratiometric sensors used in this work were ORNEX4 (orange-red-labeled annexin A4), CYCaMIIα, and PM-CKAR (*14*) (Figure 1, panel a). mCherry and mOrange fluorescent proteins were employed to flank annexin A4 to form the ORNEX4 sensor. CYCaMIIα had the CaMKIIα sequence flanked by EYFP and ECFP. This design is similar to the CaMKII sensor "Camui", described to monitor activation of CaMKII in neurons (*15*). PM-CKAR is a plasma membrane-associated cyan−yellow sensor used to report PKC activity (*14*).

Experiments were performed by expressing the sensors in N1E-115 neuroblastoma cells. Ionomycin was used to reproducibly

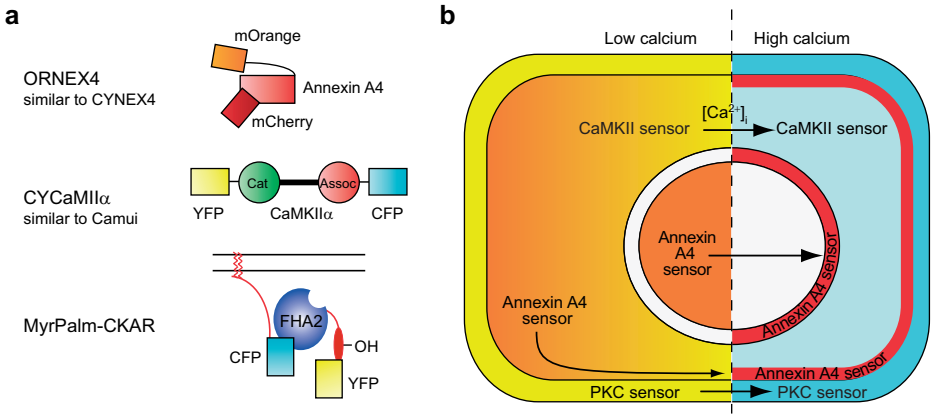

Figure 1. The concept of simultaneous triple ratiometric FRET measurements. a) Sensors that can be spectrally and/or spatially resolved. ORNEX is an mOrange−mCherry annexin A4 sensor that exhibits FRET upon assembly of annexin molecules under the plasma membrane. CYCaMIIα is an ECFP-EYFP-based sensor for CaMKIIα, and PM-CKAR is a plasma-membrane-associated mCFP−mYFP PKC-sensitive FRET sensor. b) Schematic view of a cell expressing the three sensors before (left) and after calcium stimulation (right). A decrease in FRET by the PKC and CaMKIIα sensors is observed at the plasma membrane and in the cytosol, respectively. Annexin A4 sensor exhibits increased FRET upon translocation to the plasma and the nuclear membrane.

elevate intracellular calcium levels, ensuring the full response of all three sensors when individually expressed (see Supplementary Figure 1). The sensors were then cotransfected into N1E-115 cells. The aim was to record cyan, yellow, orange, and red emission and to calculate the respective emission ratios and their changes in response to elevation of intracellular calcium levels (Figure 1, panel b). For this purpose, images were acquired on a Leica TCS SP2 AOBS microscope with an HCX PL APO lbd.BL 63.0x 1.40 oil objective at 22 °C. First we tested a combination of CYCaMIIα and ORNEX4. CFP was excited with a 405 nm laser, and emission was sampled between 470 and 510 nm. Sensitized YFP emission was collected between 520 and 540 nm. mOrange was excited with a 561 nm laser, and emission was sampled from 565 to 600 nm and mCherry from 610 to 650 nm. Background-subtracted YFP and CFP images were smoothed with a median filter and thresholded. For each pixel in the image, YFP intensity values were then divided by CFP intensity values using ImageJ (http://rsb.info.nih.gov/ij/). In the same way, the mCherry/mOrange ratio was calculated after background subtraction, image smoothing, and thresholding. Instead of exciting mOrange at 561 nm, we also tried a 532 nm laser. However, bleed-through correction was necessary in these experiments due to direct YFP excitation and the corresponding emission into mOrange and mCherry channels. This resulted in more noisy and less reproducible ORNEX4 traces (data not shown).

By imaging CaMKIIα activity and annexin membrane assembly by time-lapse microscopy, YFP/CFP ratio changes happened earlier than responses of the ORNEX4, indicating that CaMKIIα activation preceded annexin A4 self-association (Figure 2, panel a). A similar result was obtained when the PKC sensor PM-CKAR was used in parallel to the annexin A4 sensor (Figure 2, panel b).

Next, PM-CKAR and CYCaMIIα were employed in parallel. Because both sensors consist of cyan and yellow proteins, only two channels were measured in this case and only one ratio image calculated. Nevertheless, as a result of the

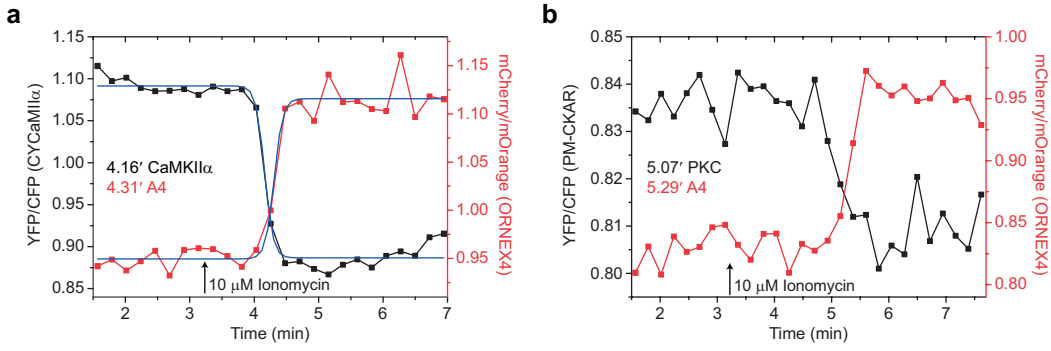

Figure 2. Dual ratiometric FRET measurements in N1E-115 cells. a) FRET ratio analysis of CYCaMIIα and ORNEX4 in a single N1E-115 cell. Half-times of enzyme activation and annexin A4 self-association/translocation were obtained from sigmoidal fits (blue line) of individual curves and are indicated in each graph throughout. b) FRET ratio analysis of PM-CKAR and ORNEX4 in a single N1E-115 cell. The results are representative of at least three independent experiments.

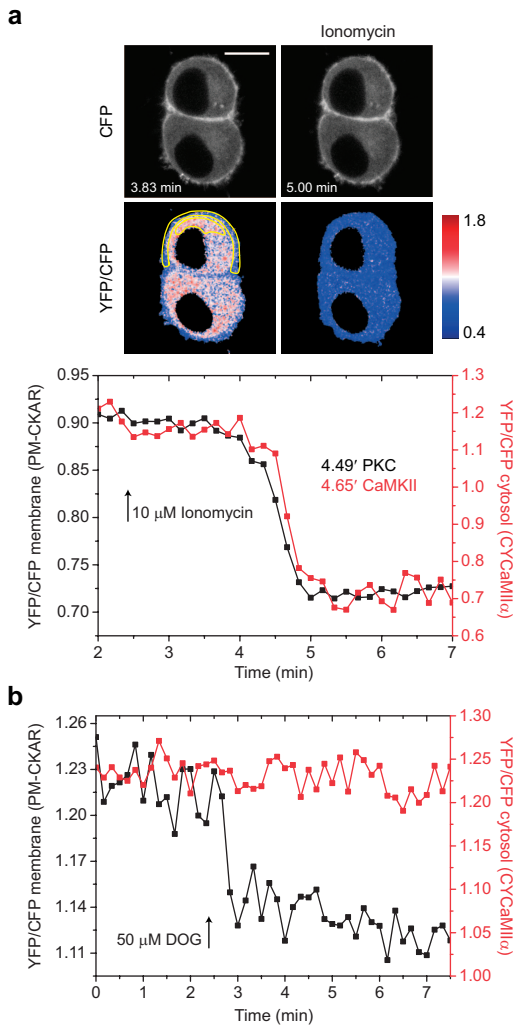

Figure 3. Simultaneous measurements of CaMKIIα and PKC activation in N1E-115 cells. a) N1E-115 cells expressing PM-CKAR and CYCaMIIα. CFP images before and after ionomycin stimulation are shown demonstrating distinct membrane and cytosolic distribution of the two sensors. YFP/CFP ratio images are shown with the corresponding LUT. The graph depicts FRET ratio changes measured in selected regions of interest indicated by yellow lines in the membrane and the cytosol of one of the displayed cells. Bar, 15 μm. b) A similar experiment as before, but the cells were stimulated with the specific PKC activator DOG. While PKC was activated, CaMKIIα remained unaffected. The results are representative of at least three independent experiments.

distinct cellular localization of the sensors, separate information from each reporter was extracted from the images. PKC activation was measured within a region of interest at the plasma membrane, and CaMKIIα activation from one in the cytosol (Figure 3, panel a). Experiments with individually expressed sensors demonstrating their localization and a more detailed description of the quantification can be found in Supporting Information. In more than half of the experiments, PKC appeared to be activated earlier than CaMKIIα. In the remaining experiments, CaMKIIα activation minimally preceded PKC activation (see below). Because both sensors responded with a FRET decrease, we wanted to confirm that spatial separation was efficient. We used 1,2-di-*O*-octanoyl-*sn*-glycerol (DOG) as a specific activator of PKC. This stimulus induced no response of CYCaMIIα while the PM-CKAR emission ratio change was evident in the plasma membrane (Figure 3, panel b). On the other hand, treating cells with Gö6983, a specific PKC inhibitor (*16*), prior to ionomycin led to full CaMKIIα activation but gave reduced PKC activity (see Supplementary Figure 2).

Subsequently, all three ratiometric FRET sensors were cotransfected. Data were collected, and ratio images were calculated and analyzed as described above (Figure 4, panel a). The timing of events followed that of the two-parameter experiments. Calculated together from all experiments using half-times of sensor activation, PKC was activated prior to CaMKIIα in 27 cells with the mean advantage (±SD) of 10.8 ± 8.6 s. CaMKIIα was 6.3 ± 5.7 s ahead of PKC in 22 cells. Both processes clearly preceded annexin A4 self-association 9.3 ± 8.6 s (n = 27 cells). The order of events can be correlated to calcium binding parameters of the proteins relevant to sensor activation. Calcium binding affinity of CaMKII activator calmodulin (0.5–5 μM) (*17*) can be as low as the calcium concentration required for half-maximal PKCα binding to phospholipids (0.3–0.7 μM) (*18*). The latter event is necessary for phosphorylation of PM-CKAR. On the other hand, half-maximal binding of annexin A4 to phospholipids is known to occur at higher calcium concentration (2.4–6 μM) (*19*). Accordingly, annexin A4 translocation was the most delayed of the observed events.

The experiment described above demonstrates that three or more ratiometric sensors can be monitored in parallel in a single cell, as long as their signals can be spectrally and/or spatially resolved. Finally, a four-parameter experiment was performed. Here, the calcium sensor Fura red was used to detect intracellular calcium changes in addition to the three parameters monitored before. Prior to imaging, 7.5 μM Fura red/AM (Molecular Probes, Invitrogen) was loaded into cells for 30 min. Fura red was excited with the 405 nm laser line also used to excite CFP, and emission was sampled from 610 to 650 nm. Using these settings Fura red fluorescence increases upon calcium binding. Care was taken not to overload the cells with Fura red. As a result only a negligible bleed-through of Fura red into CFP and YFP channels, not affecting the calculation of YFP/CFP ratio, was observed. However, we were unable to calculate mCherry/mOrange ratio in experiments with Fura red loaded N1E-115 cells. Contribution of Fura red to the mCherry channel was too significant and could not be separated. Therefore, annexin A4 (as ORNEX4)

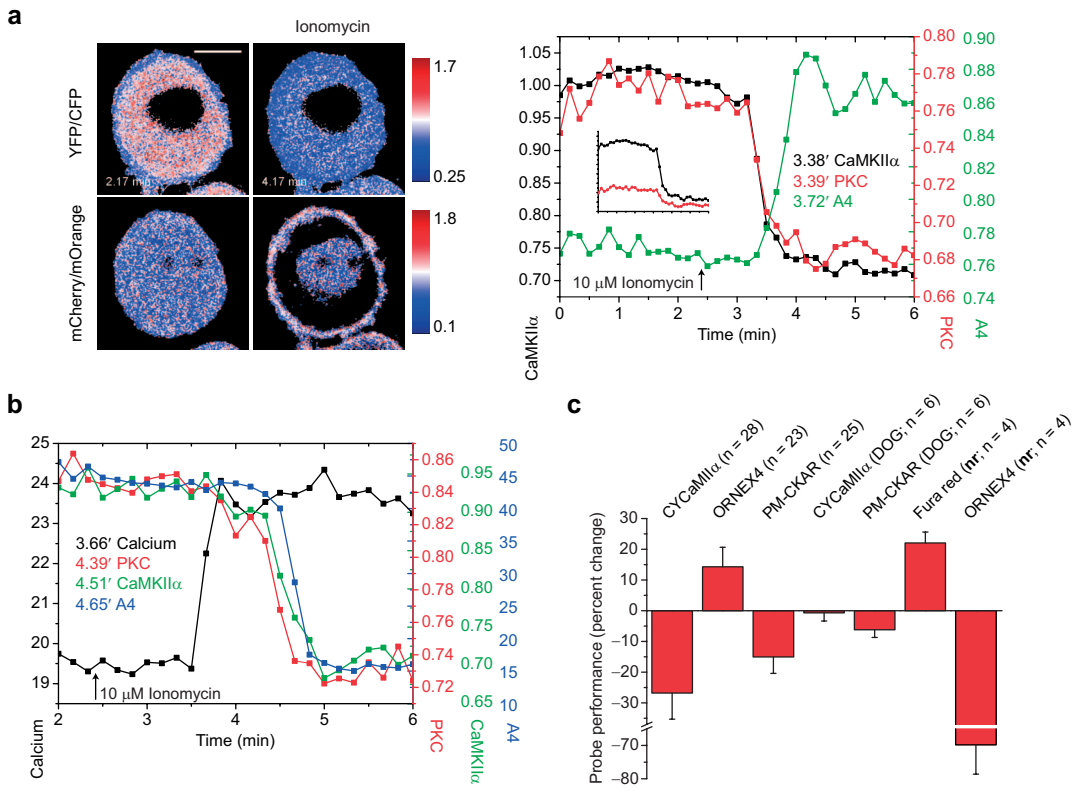

Figure 4. Simultaneous multiple time-lapse ratiometric FRET measurements in N1E-115 cells. a) YFP/CFP and mCherry/mOrange ratio images of an N1E-115 cell expressing three FRET sensors are shown. In addition, normalized FRET ratio curves are depicted in the large graph. The inserted graph shows the two kinase traces without normalization. Bar, 10 μm. b) A four-parameter experiment. Following the rise in calcium, PKC and CaMKIIα are activated and annexin A4 translocation is induced. Annexin A4 levels in the cytosol and calcium levels are nonratiometric, and fluorescence values are on an arbitrary scale. All results are representative of at least three independent experiments. c) Probe performance calculated from two-, three-, and four-parameter experiments. Shown is the mean FRET ratio change ± SD or mean change in fluorescence intensity ± SD in the case of Fura red and ORNEX4 translocation measurement in the four-parameter experiments. The numbers in brackets indicate the number of cells used to calculate the mean (nr = nonratiometric). See Supplementary Figure 3 for probe performances calculated for each individual set of experiments.

translocation was measured as loss of mOrange fluorescence in the cytosol. The experiment confirmed the previous results. At 0.5 min (38.5 ± 6.8 s, n = 4) after the initial rise in calcium levels, PKC and CaMKIIα were activated, followed by annexin A4 translocation (Figure 4, panel b). The performance of FRET sensors was constant and similar in all two-, three-, and four-parameter experiments (Figure 4, panel c).

In summary, we designed ORNEX4, a FRET sensor utilizing mOrange and mCherry fluorescent proteins, which successfully reported annexin A4 translocation and self-association. Dual and triple ratiometric FRET experiments were performed and demonstrated that following calcium stimulation both CaMKIIα and PKC activation precede annexin A4 self-association. On average, PKC was activated slightly prior to CaMKIIα. Four-parameter imaging allowed visualization of calcium levels and three different calcium-dependent events in one single cell. These results support the observation that stimulation of intracellular calcium levels leads to transient CaCC induction (*13*). The transient character of the response might be attributed to activation by CaMKII and PKC followed by inhibition through annexin A4, at least when high calcium levels are involved (*11, 12*). Although overexpression of genetically encoded sensors may result in buffering effects and influence the biology of the cells (*3, 4*), this phenomenon was not expected to influence the results of this study, since the three parameters measured by FRET are independent of each other. Nevertheless, it should be noted that buffering effects of multiple probes expressed in a single cell may influence the result when the events of interest are depending on each other, such as subsequent elements in a signaling cascade.

We demonstrated that multiple ratiometric FRET experiments can be used to address important questions in the timing of intracellular events. Sequential response patterns can be analyzed from these multiparameter experiments, which will help to unravel complex signaling mechanisms. With more sensors developed in the future, especially

those covering red parts of the usable spectra and/or occupying specific cellular localizations, simultaneous visualization of more parameters, possibly entire signaling cascades, might eventually become possible. This will have a profound impact on understanding the orchestrated timing of intracellular events. In addition, multiparameter imaging in living cells will be useful for high content screening of drug candidates in the future (*20*).

METHODS

Cloning. *pmCherry-N1-annexin A4.* mCherry was amplified by PCR using the following primers: forward 5′-TTA TTC ACC GGT CGC CAC CAT GGT GAG CAA GGG CGA GGA G-3′, reverse 5′-ATA ATC GCG GCC GCT TTA CTT GTA CAG CTC GTC CAT GCC GCC-3′. The ECFP sequence in the pECFP-N1-annexin A4 (*9*) vector was then replaced with the mCherry sequence using AgeI and NotI restriction enzymes to give the annexin A4-mCherry fusion.

pmOrange-annexin A4-mCherry. To construct the mOrange-annexin A4-mCherry double fusion (ORNEX4), mOrange was amplified using the following primers: forward 5′-GGA CTC AGA TCT CGC CAC CAT GGT GAG CAA GGG CGA GGA G-3′, reverse 5′-GTG GCG AGA ATT CGC TTG TAC AGC TCG TCC ATG CCG CC-3′. The PCR product was digested with BglII and EcoRI and ligated into the pmCherry-N1-annexin A4 vector.

pEYFP-CaMKIIα-ECFP. Rat CaMKIIα was amplified by PCR using the following primers: forward 5′-AAT CTT CGA ATT CTC GCC ACC ATG GCT ACC ATC ACC TGC ACC CGA TTC-3′, reverse 5′-TTA AAT ACC GGT GGA TCC CGA CAA TGG GGC AGG ACG GAG GGC GC-3′. The annexin A4 sequence in pEYFP-annexin A4-ECFP (*9*) was then replaced with the CaMKIIα sequence using EcoRI and AgeI restriction sites to give EYFP-CaMKIIα-ECFP fusion (CYCaMIIα).

Cell Culture and Transfection. N1E-115 cells were passaged and maintained in DMEM supplemented with 10% FBS and 0.1 mg mL^{-1} primocin. For imaging experiments, cells were plated in 35-mm MatTek chambers (MatTek Corporation) and transfected at 50% confluency with FuGENE 6 reagent (Roche). Transfections were performed in Opti-MEM (Gibco) according to the manufacturer's instructions. For multiple transfections, equal amounts of DNA were used for each sensor. Cells were washed 12–24 h after transfection and incubated in imaging medium (20 mM Hepes, pH 7.4, 115 mM NaCl, 1.2 mM $CaCl_2$, 1.2 mM $MgCl_2$, 1.2 mM K_2HPO_4, 2 g L^{-1} D-glucose) at 37 °C with 5% CO_2 for 30 min before imaging. A DMSO stock of ionomycin (Calbiochem) was prepared, and ionomycin was prediluted in imaging medium before it was carefully added to the dish. DOG and Gö6983 were from Calbiochem, and Fura red was from Molecular Probes (Invitrogen).

Equipment and Settings. All experiments were performed on a Leica TCS SP2 AOBS microscope (Leica Microsystems). We used an HCX PL APO lbd.BL 63.0x 1.40 oil objective. Pinhole was half-opened in all experiments (2.62 airy). Excitation and emission settings were kept constant. CFP–YFP sensors: 405 nm excitation, CFP emission 470–510 nm, YFP emission 520–540 nm. mOrange–mCherry sensor imaging in parallel to CFP–YFP sensors: 561 nm excitation; mOrange emission 565–600 nm, mCherry emission 610–650 nm. mOrange–mCherry sensor measured individually: 515/532/561 nm excitation, mOrange emission 560/580–600 nm, mCherry emission 610–650 nm. Fura red: 405 nm excitation, emission 610–650 nm. Laser power and PMT gain were adjusted from experiment to experiment. Images were taken in 8-bit mode, with 2–4 line averaging and 7–15 s between frames.

Image Processing and Data Analysis. All image processing and calculations were performed using ImageJ (http://rsb.info.nih.gov/ij/). Background levels were measured outside cells and subtracted globally. Median filter (1–2 pixels) was used for image smoothening. A low threshold had to be applied before ratio calculation to avoid calculation artifacts. Blue-white-red LUT was applied to ratio images, and brightness/contrast was adjusted for better visualization of small ratio changes. Sigmoidal fits were used to obtain half-times of activation of individual probes and their average initial and final FRET ratios (or fluorescence intensities). Those values were used to calculate the difference in timing of probe activation and probe performance.

Acknowledgment: We thank T. Zimmermann and S. Terjung of EMBL's Advanced Light Microscopy Facility for technical advice and H. Stichnoth for cultured cells, A. Newton (UCSD) for PM-CKAR, R. Tsien (UCSD) for mOrange and mCherry, T. Meyer (Stanford) for CaMKIIα cDNA. We thank D. Gadella (Amsterdam) for critically reading the manuscript. Partial funding was provided by E. U. grant LSHG-CT-2003-503259.

Supporting Information Available: This material is available free of charge *via* the Internet.

REFERENCES

1. Chudakov, D. M., Lukyanov, S., and Lukyanov, K. A. (2005) Fluorescent proteins as a toolkit for in vivo imaging, *Trends Biotechnol. 23*, 605–613.
2. Giepmans, B. N., Adams, S. R., Ellisman, M. H., and Tsien, R. Y. (2006) The fluorescent toolbox for assessing protein location and function, *Science 312*, 217–224.
3. Miyawaki, A. (2003) Visualization of the spatial and temporal dynamics of intracellular signaling, *Dev. Cell 4*, 295–305.
4. Zhang, J., Campbell, R. E., Ting, A. Y., and Tsien, R. Y. (2002) Creating new fluorescent probes for cell biology, *Nat. Rev. Mol. Cell. Biol. 3*, 906–918.
5. Pollok, B. A., and Heim, R. (1999) Using GFP in FRET-based applications, *Trends Cell. Biol. 9*, 57–60.
6. Schultz, C., Schleifenbaum, A., Goedhart, J., and Gadella, T. W., Jr. (2005) Multiparameter imaging for the analysis of intracellular signaling, *Chembiochem 6*, 1323–1330.
7. Galperin, E., Verkhusha, V. V., and Sorkin, A. (2004) Three-chromophore FRET microscopy to analyze multiprotein interactions in living cells, *Nat. Methods 1*, 209–217.
8. Peyker, A., Rocks, O., and Bastiaens, P. I. (2005) Imaging activation of two Ras isoforms simultaneously in a single cell, *Chembiochem 6*, 78–85.
9. Piljic, A., and Schultz, C. (2006) Annexin A4 self-association modulates general membrane protein mobility in living cells, *Mol. Biol. Cell 17*, 3318–3328.
10. Goedhart, J., Vermeer, J. E., Adjobo-Hermans, M. J., van Weeren, L., and Gadella, T. W. (2007) Sensitive detection of p65 homodimers using red-shifted and fluorescent protein-based FRET couples, *PLoS ONE 2*, e1011.
11. Chan, H. C., Kaetzel, M. A., Gotter, A. L., Dedman, J. R., and Nelson, D. J. (1994) Annexin IV inhibits calmodulin-dependent protein kinase II-activated chloride conductance. A novel mechanism for ion channel regulation, *J. Biol. Chem. 269*, 32464–32468.
12. Fuller, C. M., and Benos, D. J. (2000) Ca^{2+}-activated Cl^- channels: a newly emerging anion transport family, *News Physiol. Sci. 15*, 165–171.
13. Rudolf, M. T., Dinkel, C., Traynor-Kaplan, A. E., and Schultz, C. (2003) Antagonists of myo-inositol 3,4,5,6-tetrakisphosphate allow repeated epithelial chloride secretion, *Bioorg. Med. Chem. 11*, 3315–3329.
14. Violin, J. D., Zhang, J., Tsien, R. Y., and Newton, A. C. (2003) A genetically encoded fluorescent reporter reveals oscillatory phosphorylation by protein kinase C, *J. Cell. Biol. 161*, 899–909.
15. Takao, K., Okamoto, K., Nakagawa, T., Neve, R. L., Nagai, T., Miyawaki, A., Hashikawa, T., Kobayashi, S., and Hayashi, Y. (2005) Visualization of synaptic Ca^{2+}/calmodulin-dependent protein kinase II activity in living neurons, *J. Neurosci. 25*, 3107–3112.
16. Gschwendt, M., Dieterich, S., Rennecke, J., Kittstein, W., Mueller, H. J., and Johannes, F. J. (1996) Inhibition of protein kinase C mu by various inhibitors. Differentiation from protein kinase c isoenzymes, *FEBS Lett. 392*, 77–80.
17. Chin, D., and Means, A. R. (2000) Calmodulin: a prototypical calcium sensor, *Trends Cell Biol. 10*, 322–328.
18. Corbalan-Garcia, S., Rodriguez-Alfaro, J. A., and Gomez-Fernandez, J. C. (1999) Determination of the calcium-binding sites of the C2 domain of protein kinase Calpha that are critical for its translocation to the plasma membrane, *Biochem. J. 337*, 513–521.
19. Raynal, P., and Pollard, H. B. (1994) Annexins: the problem of assessing the biological role for a gene family of multifunctional calcium- and phospholipid-binding proteins, *Biochim. Biophys. Acta 1197*, 63–93.
20. Lang, P., Yeow, K., Nichols, A., and Scheer, A. (2006) Cellular imaging in drug discovery, *Nat. Rev. Drug Discovery 5*, 343–356.